Published OnlineFirst October 10, 2018; DOI: 10.1158/1535-7163.MCT-18-0243

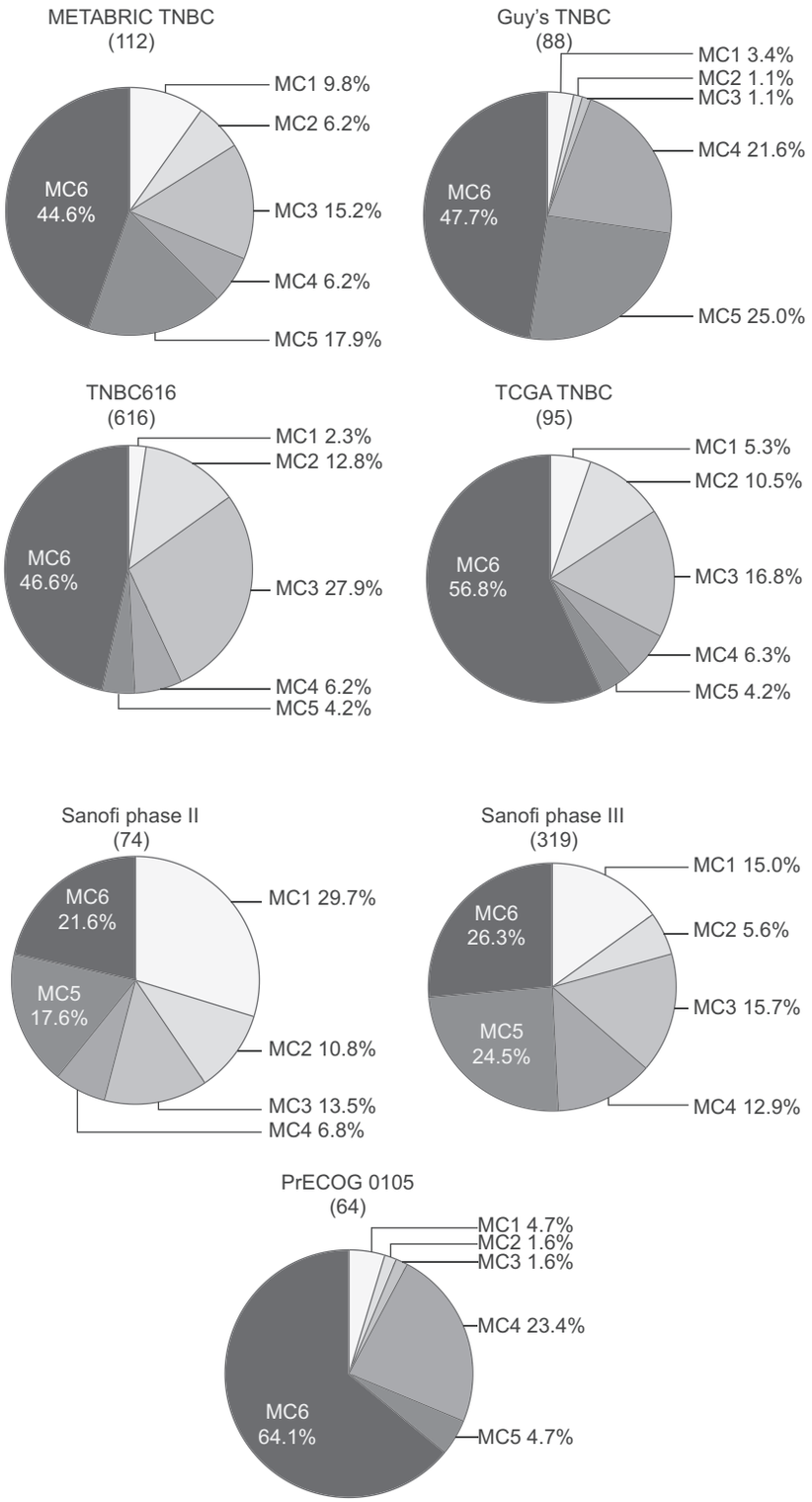

Figure 2.

TNBC cohorts classified using the *METABRIC-set 15* four-gene decision tree signature. Pie charts illustrating the proportion of the MC subtypes in four primary invasive TNBC cohorts, namely METABRIC TNBC, Guy's TNBC, TNBC616, and TCGA TNBC, as well as three clinical TNBC studies, including Sanofi phase II, Sanofi phase III, and PrECOG 0105. The total number of tumors in each cohort is listed in brackets. The percentage for each subgroup is shown next to the respective pies.

basal-like cases (100%, $P = 2e{-}08$, Fisher exact test), although only 57% of the basal-like TNBCs were classified as MC6. MC1-TNBCs were enriched for Luminal A (36%, $P = 3e{-}04$, Fisher exact test) and Normal-like (36%, $P = 3e{-}03$, Fisher exact test), and MC2-TNBCs for HER2-enriched (57%, $P = 2e{-}03$, Fisher exact test). TNBCs of the remaining three MC subtypes fell across all PAM50 subtypes. Except for three TNBCs, MC6-TNBCs belonged to the IntClust 10 group (78%, $P = 1e{-}02$, Fisher exact

Published OnlineFirst October 10, 2018; DOI: 10.1158/1535-7163.MCT-18-0243

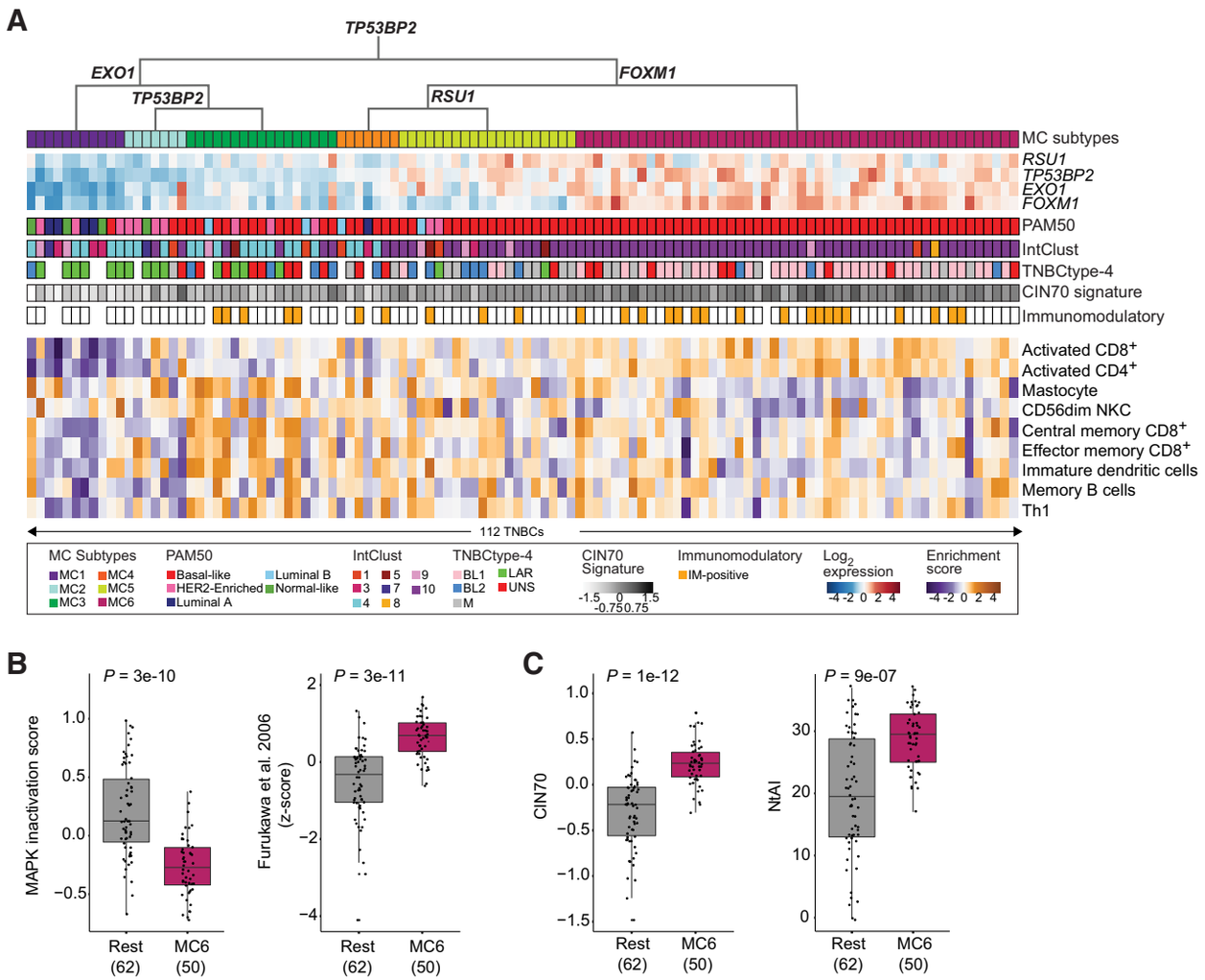

Figure 3.

Molecular characterization of the MC subtypes in METABRIC TNBC. **A,** The four-gene decision tree underlying the MC subtypes is shown, followed by a heatmap representing the expression levels of the four modulatory genes. The colored bars represent sample-specific characteristics, including PAM50, IntClust, TNBCtype-4, CIN70 signature, and the immunomodulatory status. The heatmap at the bottom illustrates the enrichment of immune gene signatures. **B,** (left) MAPK inactivation scores, calculated by summarizing the expression levels of *DUSP4, DUSP5, DUSP6, DUSP10,* and *SPRED2*, in MC6-TNBCs (magenta) and the remaining TNBCs (gray). Significance was assessed using Wilcoxon rank-sum tests. (right) Z-scores for the *DUSP6* gene set were obtained using ssGSEA. Significance was assessed using a Wilcoxon rank-sum test. **C,** Boxplots displaying the CIN70 signature (left) and NtAI (right) in MC6-TNBCs (magenta) and the remaining TNBCs (gray). Significance was assessed using Wilcoxon rank-sum tests.

test), whereas TNBCs of other MC subtypes were classified mostly as IntClust 4, 5, 3, and 1, although no significant enrichments were observed. MC6-TNBCs were found to be enriched for the BL1 subtype (61%, $P = 1e{-}06$, Fisher exact test), whereas MC1-TNBCs and MC2-TNBCs were primarily of the LAR subtype (86% and 67%, $P = 1e{-}04$ and $1e{-}02$, respectively, Fisher exact test). Thus, the MC subtypes diverged from established breast cancer classifications

MC subtypes differ in their immune gene enrichment. On the basis of Lehmann's immunomodulatory (IM) classification (12), 37% of the MC6-TNBCs were IM-positive, MC1- and MC2-TNBCs were exclusively IM-negative, and MC3-, MC4- and MC5-TNBCs were mostly IM-negative (74%; Fig. 3A). Next, we performed a gene set enrichment analysis (38) on gene expression data from METABRIC TNBC to further deconvolute immune cell enrichment across the MC subtypes. Using 28 different immune gene sets (39), activated $CD4^+$ and $CD8^+$ immune signatures were found enriched in MC6-TNBCs ($Q = 3e{-}08$, and $1e{-}04$, respectively, Mann–Whitney *U* test), and low in MC1-TNBCs ($Q = 2e{-}05$ and $1e{-}05$, Mann–Whitney *U* test; Fig. 3A; Supplementary Table S16). MC6-TNBC had lower mastocytes and $CD56^{dim}$ natural killer cell activation in comparison with other MC subtypes ($Q = 5e{-}03$, and $3e{-}02$, respectively, Mann–Whitney *U* test). In MC3-TNBCs, increased central memory $CD8^+$, effector memory $CD8^+$, and immature dendritic cells expression levels were observed ($Q = 4e{-}02$, $4e{-}02$, and $4e{-}02$, respectively, Mann–Whitney *U* test). MC2-TNBCs had reduced expression of the

Published OnlineFirst October 10, 2018; DOI: 10.1158/1535-7163.MCT-18-0243

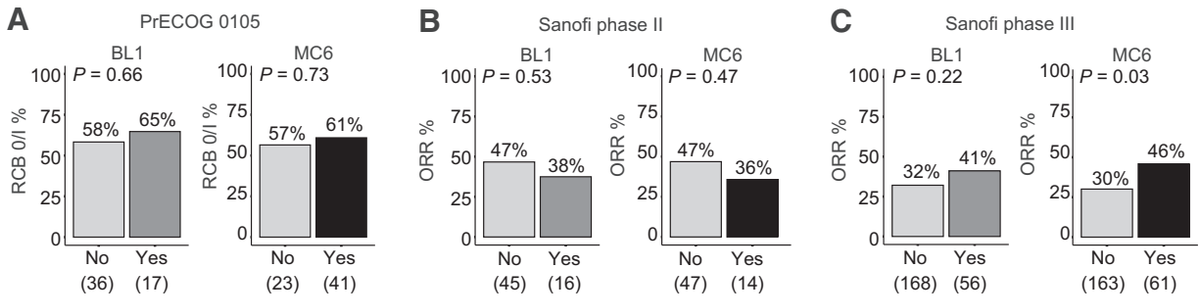

Figure 4.

Response rates for the MC6 and BL1 subtypes in clinical trials. **A,** Response to neoadjuvant platinum-based chemotherapy, as assessed by the RCB index, in BL1-TNBCs and MC6-TNBCs obtained from the PrECOG 0105 clinical trial. ORR in Sanofi phase II (**B**) and Sanofi phase III (**C**). Response rates are dichotomized by being BL1 or not (left), and MC6 or not (right). Subtypes were assessed as predictors of treatment response using a multivariate logistic regression, by including age and race for Sanofi II, and age, race, and grade for Sanofi III into the models.

memory B-cell signature ($Q = 4e{-}02$, Mann–Whitney *U* test), whereas in MC1-TNBCs, Th1 expression was reduced ($Q = 4e{-}02$, Mann–Whitney *U* test). This clearly demonstrates a variety of immune cell features across the MC subtypes.

Pathway deregulation in MC subtypes. *DUSP4*, *DUSP5*, *DUSP6*, *DUSP10*, and *SPRED2* were amongst the *METABRIC-set 15 gene set* (Fig. 1D; Supplementary Table S8) and are involved in the negative regulation of the MAPK signaling pathway. We investigated their expression levels across the MC subtypes and found that MC6-TNBCs had the lowest expression of these genes in comparison with the other subtypes ($P < 0.05$, Mann–Whitney *U* test; Fig. 3B; Supplementary Fig. S3A). Genomic regions encompassing *DUSP4*, *DUSP5*, and *DUSP6* were deleted (Supplementary Table S17), potentially resulting in decreased expression levels. To further corroborate the lack of negative regulation of MAPK inactivation, a set of genes previously reported under control of this inhibitory mechanism (40) was interrogated in the MC subtypes and found increased in MC6-TNBCs compared with TNBCs of other MC subtypes ($P < 0.05$, Mann–Whitney *U* test; Fig. 3B; Supplementary Fig. S3B). These results demonstrate the highly selective features of MC6-TNBCs.

In MC5-TNBCs, genes highly expressed were enriched for ErbB signaling ($Q = 6e{-}03$, Hypergeometric test), particularly through the EGFR pathway ($P = 1e{-}02$, Fisher exact test). MC4-TNBCs were enriched for PI3K/Akt signaling ($Q = 5e{-}03$, Hypergeometric test) and DNA replication ($P = 2e{-}02$, Fisher exact test). Although not enriched for Lehmann's IM classification, many genes upregulated in MC3-TNBCs are involved in innate and adaptive immune response ($P = 7e{-}04$ and $1e{-}03$, respectively, Fisher exact test), and chemokine signaling ($Q = 3e{-}03$, Hypergeometric test). MC2-TNBCs were enriched for metabolic processes ($Q = 2e{-}28$, Hypergeometric test), and MC1-TNBCs for steroid hormone–mediated signaling ($P = 3e{-}02$, Fisher exact test), particularly estrogen and androgen receptor signaling ($P = 7e{-}04$ and $2e{-}02$, respectively, Fisher exact test). The unique pathway activities underlying the MC subtypes further demonstrate the molecular complexity of TNBC and further strengthen our TNBC classification.

Increased levels of telomeric allelic imbalanced aberrations in MC6-TNBCs. Next, we investigated the levels of genomic instability. MC6-TNBCs showed significantly higher levels of chromosomal instability ($P < 0.05$, Mann–Whitney *U* test; Fig. 3C; Supplementary Fig. S3C) as defined by the CIN70 gene expression signature (16, 41). MC1-TNBCs had the lowest levels of chromosomal instability. To further decipher this genomic instability, we investigated diverse genomic instability measurements based on copy number data (17, 18). MC6-TNBCs displayed a high burden of allelic imbalanced aberrations in their telomeres ($P = 9e{-}07$, Mann–Whitney U test; Fig. 3C). MC5-TNBCs exhibited a medium burden. In contrast, the remaining MC subtypes did not harbor specific types of copy number aberrations.

MC6 identifies TNBCs responsive to platinum-based chemotherapy in Sanofi phase III clinical trial. Given the selective features of MC6-TNBCs, we next assessed whether this subtype carried any predictive value in treatment response to DNA-damaging agents. Using three clinical trials (Fig. 1A), TNBCs from each cohort were dichotomized as either being MC6-TNBCs or non-MC6 (referred to as remaining TNBCs). We included the TNBCtype-4 classification as a comparator, as BL1-TNBCs were previously shown to be responsive to neoadjuvant chemotherapy (12). In the neoadjuvant PrECOG 0105 trial, the RCB 0/I pathological response rate in BL1-TNBCs (11/17, 65%) was similar to that of MC6-TNBCs (25/41, 61%; Fig. 4A). However, of the 64 patients enrolled in the PrECOG 0105 trial, the MC6 subtype identified 39% of the responders with an accuracy of 55%, in contrast to the BL1 subtype, identifying 17%, with an accuracy of 41%. In the metastatic TNBC Sanofi phase II trial, neither the BL1 nor the MC6 subtype was predictive of the overall response rate (ORR; Fig. 4B; Supplementary Table S18). However, in the metastatic TNBC Sanofi phase III trial, the MC6 subtype was a significant predictor of treatment response in a multivariate model [OR = 2.41, confidence interval (CI) = 1.01 to 5.81, $P < 0.05$], with an ORR in MC6-TNBCs of 46% (28/61), compared with an ORR of 30% (49/163) in the remaining TNBCs (Fig. 4C). The ORR in BL1-TNBCs was 41% (23/56), as compared with 32% (54/168) in the remaining TNBCs. In contrast to BL1, the MC6 subtype did reach significance in the univariate and in the multivariate model (OR = 1.78, CI = 0.76 to 4.19, $P = 0.18$; Supplementary Table S19).

MC6 cell lines are sensitive to cisplatin. To test the hypothesis that MC6-TNBCs are responsive to platinum-based chemotherapeutics, we exploited drug sensitivity profiles of 16 TNBC tumor cell

Published OnlineFirst October 10, 2018; DOI: 10.1158/1535-7163.MCT-18-0243

lines generated as part of the GDSC project (33). We found that the median AUC of cisplatin in the MC6 TNBC cell lines ($n = 4$) was 0.89, compared with 0.92 in cell lines from other MC subtypes ($n = 11$; $P = 5.6e{-}02$, Mann–Whitney U test), suggesting an enhanced sensitivity to platinum salts in the MC6 subtype. With the aim of identifying novel alternative therapeutic sensitivities, we also assessed the associations between >200 GDSC drug response profiles and the MC6 subtype (Supplementary Table S20). We found that among the GDSC drug sensitivity profiles, MC6-TNBC cell lines displayed the greatest sensitivity to CCT007093 (42), a small-molecule inhibitor of the DNA damage–activated phosphatase, PPM1D ($P = 7.7e{-}03$, Mann–Whitney U test, Supplementary Fig. S4; ref. 43).

Discussion

With the purpose of classifying molecular heterogeneous TNBCs into clinically relevant subtypes, our multi-omics integrative approach differs from previously published methods (10–13). Our classification was constructed using data exclusively from TNBCs, strengthening the exploration of their molecular complexity in more detail. Robustness of our approach was increased by applying the CONEXIC algorithm (34) to two independent TNBC cohorts to then identify concurrent gene sets and modulatory genes. *Guy's-set 33* and *METABRIC-set 15* shared similarities in both their gene set and modulatory genes. The latter represented well-known cancer-associated genes potentially contributing to tumor progression, and thereby substantiating our analytical approach to identify candidate drivers with effects on gene expression patterns. However, upon validation of both decision trees, only *METABRIC-set 15* was taken forward due to the consistently reproducible MC subtypes. Of note, the molecular features of primary tumors of patients that will be developing metastasis seem to be distinct, as was reflected by the change in proportion of the MC1 and MC6 subtype between nontrial and metastatic TNBC cohorts. The MC6 subtype identified patients with metastatic TNBC who showed improved response to platinum-based chemotherapy in the Sanofi phase III, but not in the neoadjuvant PrECOG 0105 trial (5). In early-stage TNBCs, which are more likely to respond to platinum-based chemotherapy, the MC6 subtype is not able to differentiate between those that do, and do not respond to this treatment. However, in the metastatic setting, where patients are less responsive to platinum-based chemotherapy, MC6 appears to be more discriminative as a predictor. In contrast, genomic signatures lack predictive value in the metastatic setting (22, 23).

The four-gene decision tree signature consists of *TP53BP2*, *RSU1*, *FOXM1*, and *EXO1*. The expression of *TP53BP2*, a known regulator of apoptosis and cell growth, has been reported to be copy number dependent, and is associated with poor response to chemotherapy in TNBC (14). *RSU1*, Ras suppressor-1, is involved in the RAS signal transduction pathway and was proposed as a biomarker for metastasis in breast cancers (44). The proto-oncogenic transcription factor *FOXM1* has frequently been shown to mediate cell proliferation, survival, migration, progression, and tumorigenesis in TNBC (45); can modulate cisplatin sensitivity by regulating the expression of *EXO1* in ovarian cancer (46); and is part of a recently identified KRAS-associated signature in colorectal cancer (47). All four genes provide biological rationales for being good candidates for classification approaches.

To further substantiate the finding that MC6-TNBCs were more sensitive to platinum-based chemotherapeutics, cisplatin drug response profiles were assessed across 16 TNBC cell lines categorized by MC subtypes. In line with findings from Sanofi phase III, MC6 cell lines appeared overall more sensitive to cisplatin than those of other subtypes. In addition, MC6-TNBC cell lines were found to exhibit enhanced sensitivity to CCT007093, a chemical inhibitor of PPM1D (42). In parallel, MC6-TNBC cell lines displayed lower expression of *DUSP10* and *SPRED2* as a part of the MAPK inactivation signature; both are negative regulators of p38. Loss of *DUSP4*, *DUSP5*, and *DUSP6* in TNBC has been previously reported by others (48–50). Thus, we hypothesize that the sensitivity to CCT007093 may be a result of p38-dependent cell death, thereby pointing to a potential PPM1D dependency for this group of TNBCs. Given that PPM1D modulates the activity of a series of substrates including p38, ATM, CHK1, and CHK2 (43), this association further demonstrates the connectivity between genomic instability and TNBC.

The proposed decision tree is an ideal classification approach to be performed with relative ease using other platforms, including qPCR and NanoString, due to the small number of genes required. However, there are some limitations, as in its current form, the four-gene decision tree signature relies on the distribution of each of the four genes and careful standardization experiments would need to be implemented. Furthermore, validation of our classification across independent clinical trials are warranted to investigate whether association with treatment effect to platinum-based chemotherapy is specific or rather reflects a combinatorial effect with gemcitabine in Sanofi phase III.

The management of TNBC, especially in the metastatic setting, can be complex. With single-agent chemotherapy still considered the standard-of-care, targeted therapeutic strategies are required, which will rely on appropriate biomarkers for optimal patient selection. The unique molecular features of the MC subtypes reflect the intrinsic heterogeneity of TNBC and revealed targetable pathways, such as the p38 MAPK signaling pathway in MC6-TNBC. The same subset also showed elevated levels of genomic instability in telomeric regions, a type of genomic instability, which may be the result of escaping from telomere crisis. *EXO1*, a modulatory gene, may further contribute to this process (51, 52). Futher, characterizations of the MC subtypes are warranted to establish their association with genomic signatures from whole-genome sequence data (53, 54).

In conclusion, we sought to decipher the complex nature of TNBC, with the goal of informing patient selection for current and future treatment strategies. We showed that a four-gene decision tree signature based on copy number–dependent genes classifies TNBCs into six subtypes. Given the current lack of selection criteria for TNBC patients with metastatic disease, this classification warrants further testing in randomized metastatic TNBC trials, such as TNT (22).

Disclosure of Potential Conflicts of Interest

No potential conflicts of interest were disclosed.

Disclaimer

The views expressed are those of the author(s) and not necessarily those of the NHS, the NIHR or the Department of Health.

Authors' Contributions

Conception and design: J. Quist, A.N.J. Tutt, A. Grigoriadis
Development of methodology: J. Quist, J.A. O'Shaughnessy, A. Grigoriadis

Acquisition of data (provided animals, acquired and managed patients, provided facilities, etc.): M.L. Telli, A.N.J. Tutt, A. Grigoriadis
Analysis and interpretation of data (e.g., statistical analysis, biostatistics, computational analysis): J. Quist, H. Mirza, M.C.U. Cheang, J.A. O'Shaughnessy, C.J. Lord, A. Grigoriadis
Writing, review, and/or revision of the manuscript: J. Quist, M.C.U. Cheang, M.L. Telli, J.A. O'Shaughnessy, C.J. Lord, A.N.J. Tutt, A. Grigoriadis
Administrative, technical, or material support (i.e., reporting or organizing data, constructing databases): J. Quist, A. Grigoriadis
Study supervision: A.N.J. Tutt, A. Grigoriadis

Acknowledgments

Patient samples and data were provided by King's Health Partners Cancer Biobank, London, United Kingdom, which is supported by the Experimental Cancer Medicine Centre at King's College London and the Department of Health via the National Institute for Health Research Comprehensive Biomedical Research Centre award. This article represents independent research part funded by the National Institute for Health Research (NIHR) Biomedical Research Centre at Guy's and St Thomas' NHS Foundation Trust and King's College London, and Cancer Research UK King's Health Partners Centre at King's College London. We thank Assistant Professor Uri David Akavia for his help with CONEXIC and Dr. Syed Haider for critical reading and suggestions.This work was supported by the National Institute for Health Research (NIHR) Biomedical Research Centre at Guy's and St Thomas (to J. Quist); Breast Cancer Now Programme grants at King's College London (to H. Mirza, A.N.J. Tutt, and A. Grigoriadis) and The Institute of Cancer Research (to C.J. Lord); and Cancer Research UK King's Health Partners Centre at King's College London.

The costs of publication of this article were defrayed in part by the payment of page charges. This article must therefore be hereby marked *advertisement* in accordance with 18 U.S.C. Section 1734 solely to indicate this fact.

Received March 9, 2018; revised August 2, 2018; accepted October 5, 2018; published first October 10, 2018.

References

1. Bianchini G, Balko JM, Mayer IA, Sanders ME, Gianni L. Triple-negative breast cancer: challenges and opportunities of a heterogeneous disease. Nat Rev Clin Oncol 2016;13:674–90.
2. Smid M, Wang Y, Zhang Y, Sieuwerts AM, Yu J, Klijn JG, et al. Subtypes of breast cancer show preferential site of relapse. Cancer Res 2008;68:3108–14.
3. O'Shaughnessy J, Osborne C, Pippen JE, Yoffe M, Patt D, Rocha C, et al. Iniparib plus chemotherapy in metastatic triple-negative breast cancer. N Engl J Med 2011;364:205–14.
4. O'Shaughnessy J, Schwartzberg L, Danso MA, Miller KD, Rugo HS, Neubauer M, et al. Phase III study of iniparib plus gemcitabine and carboplatin versus gemcitabine and carboplatin in patients with metastatic triple-negative breast cancer. J Clin Oncol 2014;32:3840–7.
5. Telli ML, Jensen KC, Vinayak S, Kurian AW, Lipson JA, Flaherty PJ, et al. Phase II study of gemcitabine, carboplatin, and iniparib as neoadjuvant therapy for triple-negative and BRCA1/2 mutation-associated breast cancer with assessment of a tumor-based measure of genomic instability: PrECOG 0105. J Clin Oncol 2015;33:1895–901.
6. Infante JR, Papadopoulos KP, Bendell JC, Patnaik A, Burris HA 3rd, Rasco D, et al. A phase 1b study of trametinib, an oral Mitogen-activated protein kinase kinase (MEK) inhibitor, in combination with gemcitabine in advanced solid tumours. Eur J Cancer 2013;49:2077–85.
7. Nanda R, Chow LQ, Dees EC, Berger R, Gupta S, Geva R, et al. Pembrolizumab in patients with advanced triple-negative breast cancer: phase Ib KEYNOTE-012 study. J Clin Oncol 2016;34:2460–7.
8. Silver DP, Richardson AL, Eklund AC, Wang ZC, Szallasi Z, Li Q, et al. Efficacy of neoadjuvant cisplatin in triple-negative breast cancer. J Clin Oncol 2010;28:1145–53.
9. Tutt A, Robson M, Garber JE, Domchek SM, Audeh MW, Weitzel JN, et al. Oral poly(ADP-ribose) polymerase inhibitor olaparib in patients with BRCA1 or BRCA2 mutations and advanced breast cancer: a proof-of-concept trial. Lancet 2010;376:235–44.
10. Curtis C, Shah SP, Chin SF, Turashvili G, Rueda OM, Dunning MJ, et al. The genomic and transcriptomic architecture of 2,000 breast tumours reveals novel subgroups. Nature 2012;486:346–52.
11. Lehmann BD, Bauer JA, Chen X, Sanders ME, Chakravarthy AB, Shyr Y, et al. Identification of human triple-negative breast cancer subtypes and preclinical models for selection of targeted therapies. J Clin Invest 2011;121:2750–67.
12. Lehmann BD, Jovanovic B, Chen X, Estrada MV, Johnson KN, Shyr Y, et al. Refinement of triple-negative breast cancer molecular subtypes: implications for neoadjuvant chemotherapy selection. PLoS One 2016;11:e0157368.
13. Prat A, Adamo B, Cheang MC, Anders CK, Carey LA, Perou CM. Molecular characterization of basal-like and non-basal-like triple-negative breast cancer. Oncologist 2013;18:123–33.
14. Lips EH, Michaut M, Hoogstraat M, Mulder L, Besselink NJ, Koudijs MJ, et al. Next generation sequencing of triple negative breast cancer to find predictors for chemotherapy response. Breast Cancer Res 2015;17:134.
15. Shah SP, Roth A, Goya R, Oloumi A, Ha G, Zhao Y, et al. The clonal and mutational evolution spectrum of primary triple-negative breast cancers. Nature 2012;486:395–9.
16. Birkbak NJ, Eklund AC, Li Q, McClelland SE, Endesfelder D, Tan P, et al. Paradoxical relationship between chromosomal instability and survival outcome in cancer. Cancer Res 2011;71:3447–52.
17. Watkins J, Weekes D, Shah V, Gazinska P, Joshi S, Sidhu B, et al. Genomic complexity profiling reveals that HORMAD1 overexpression contributes to homologous recombination deficiency in triple-negative breast cancers. Cancer Discov 2015;5:488–505.
18. Birkbak NJ, Wang ZC, Kim JY, Eklund AC, Li Q, Tian R, et al. Telomeric allelic imbalance indicates defective DNA repair and sensitivity to DNA-damaging agents. Cancer Discov 2012;2:366–75.
19. Abkevich V, Timms KM, Hennessy BT, Potter J, Carey MS, Meyer LA, et al. Patterns of genomic loss of heterozygosity predict homologous recombination repair defects in epithelial ovarian cancer. Br J Cancer 2012;107:1776–82.
20. Davies H, Glodzik D, Morganella S, Yates LR, Staaf J, Zou X, et al. HRDetect is a predictor of BRCA1 and BRCA2 deficiency based on mutational signatures. Nat Med 2017;23:517–25.
21. von Minckwitz G, Schneeweiss A, Loibl S, Salat C, Denkert C, Rezai M, et al. Neoadjuvant carboplatin in patients with triple-negative and HER2-positive early breast cancer (GeparSixto; GBG 66): a randomised phase 2 trial. Lancet Oncol 2014;15:747–56.
22. Tutt A, Tovey H, Cheang MCU, Kernaghan S, Kilburn L, Gazinska P, et al. Carboplatin in BRCA1/2-mutated and triple-negative breast cancer BRCAness subgroups: the TNT Trial. Nat Med 2018;24:628–37.
23. Isakoff SJ, Mayer EL, He L, Traina TA, Carey LA, Krag KJ, et al. TBCRC009: a multicenter phase II clinical trial of platinum monotherapy with biomarker assessment in metastatic triple-negative breast cancer. J Clin Oncol 2015;33:1902–9.
24. Braso-Maristany F, Filosto S, Catchpole S, Marlow R, Quist J, Francesch-Domenech E, et al. PIM1 kinase regulates cell death, tumor growth and chemotherapy response in triple-negative breast cancer. Nat Med 2016;22:1303–13.
25. Cancer Genome Atlas Network. Comprehensive molecular portraits of human breast tumours. Nature 2012;490:61–70.
26. Mendeleyev J, Kirsten E, Hakam A, Buki KG, Kun E. Potential chemotherapeutic activity of 4-iodo-3-nitrobenzamide. Metabolic reduction to the 3-nitroso derivative and induction of cell death in tumor cells in culture. Biochem Pharmacol 1995;50:705–14.
27. Symmans WF, Peintinger F, Hatzis C, Rajan R, Kuerer H, Valero V, et al. Measurement of residual breast cancer burden to predict survival after neoadjuvant chemotherapy. J Clin Oncol 2007;25:4414–22.
28. Gautier L, Cope L, Bolstad BM, Irizarry RA. affy–analysis of Affymetrix GeneChip data at the probe level. Bioinformatics 2004;20:307–15.
29. Irizarry RA, Bolstad BM, Collin F, Cope LM, Hobbs B, Speed TP. Summaries of Affymetrix GeneChip probe level data. Nucleic Acids Res 2003;31:e15.

Published OnlineFirst October 10, 2018; DOI: 10.1158/1535-7163.MCT-18-0243

30. Diskin SJ, Li M, Hou C, Yang S, Glessner J, Hakonarson H, et al. Adjustment of genomic waves in signal intensities from whole-genome SNP genotyping platforms. Nucleic Acids Res 2008;36:e126.
31. Wang K, Li M, Hadley D, Liu R, Glessner J, Grant SF, et al. PennCNV: an integrated hidden Markov model designed for high-resolution copy number variation detection in whole-genome SNP genotyping data. Genome Res 2007;17:1665–74.
32. Van Loo P, Nordgard SH, Lingjaerde OC, Russnes HG, Rye IH, Sun W, et al. Allele-specific copy number analysis of tumors. Proc Natl Acad Sci U S A 2010;107:16910–5.
33. Yang W, Soares J, Greninger P, Edelman EJ, Lightfoot H, Forbes S, et al. Genomics of Drug Sensitivity in Cancer (GDSC): a resource for therapeutic biomarker discovery in cancer cells. Nucleic Acids Res 2013;41:D955–61.
34. Akavia UD, Litvin O, Kim J, Sanchez-Garcia F, Kotliar D, Causton HC, et al. An integrated approach to uncover drivers of cancer. Cell 2010;143: 1005–17.
35. Parker JS, Mullins M, Cheang MC, Leung S, Voduc D, Vickery T, et al. Supervised risk predictor of breast cancer based on intrinsic subtypes. J Clin Oncol 2009;27:1160–7.
36. Perou CM, Sorlie T, Eisen MB, van de Rijn M, Jeffrey SS, Rees CA, et al. Molecular portraits of human breast tumours. Nature 2000;406:747–52.
37. Sorlie T, Perou CM, Tibshirani R, Aas T, Geisler S, Johnsen H, et al. Gene expression patterns of breast carcinomas distinguish tumor subclasses with clinical implications. Proc Natl Acad Sci U S A 2001;98:10869–74.
38. Subramanian A, Tamayo P, Mootha VK, Mukherjee S, Ebert BL, Gillette MA, et al. Gene set enrichment analysis: a knowledge-based approach for interpreting genome-wide expression profiles. Proc Natl Acad Sci U S A 2005;102:15545–50.
39. Angelova M, Charoentong P, Hackl H, Fischer ML, Snajder R, Krogsdam AM, et al. Characterization of the immunophenotypes and antigenomes of colorectal cancers reveals distinct tumor escape mechanisms and novel targets for immunotherapy. Genome Biol 2015;16:64.
40. Furukawa T, Kanai N, Shiwaku HO, Soga N, Uehara A, Horii A. AURKA is one of the downstream targets of MAPK1/ERK2 in pancreatic cancer. Oncogene 2006;25:4831–9.
41. Carter SL, Eklund AC, Kohane IS, Harris LN, Szallasi Z. A signature of chromosomal instability inferred from gene expression profiles predicts clinical outcome in multiple human cancers. Nat Genet 2006;38:1043–8.
42. Rayter S, Elliott R, Travers J, Rowlands MG, Richardson TB, Boxall K, et al. A chemical inhibitor of PPM1D that selectively kills cells overexpressing PPM1D. Oncogene 2008;27:1036–44.
43. Oghabi Bakhshaiesh T, Majidzadeh AK, Esmaeili R. Wip1: A candidate phosphatase for cancer diagnosis and treatment. DNA Repair (Amst) 2017;54:63–6.
44. Giotopoulou N, Valiakou V, Papanikolaou V, Dubos S, Athanassiou E, Tsezou A, et al. Ras suppressor-1 promotes apoptosis in breast cancer cells by inhibiting PINCH-1 and activating p53-upregulated-modulator of apoptosis (PUMA); verification from metastatic breast cancer human samples. Clin Exp Metastasis 2015;32:255–65.
45. Hamurcu Z, Ashour A, Kahraman N, Ozpolat B. FOXM1 regulates expression of eukaryotic elongation factor 2 kinase and promotes proliferation, invasion and tumorgenesis of human triple negative breast cancer cells. Oncotarget 2016;7:16619–35.
46. Zhou J, Wang Y, Wang Y, Yin X, He Y, Chen L, et al. FOXM1 modulates cisplatin sensitivity by regulating EXO1 in ovarian cancer. PLoS One 2014; 9:e96989.
47. Pek M, Yatim S, Chen Y, Li J, Gong M, Jiang X, et al. Oncogenic KRAS-associated gene signature defines co-targeting of CDK4/6 and MEK as a viable therapeutic strategy in colorectal cancer. Oncogene 2017;36:4975–86.
48. Balko JM, Cook RS, Vaught DB, Kuba MG, Miller TW, Bhola NE, et al. Profiling of residual breast cancers after neoadjuvant chemotherapy identifies DUSP4 deficiency as a mechanism of drug resistance. Nat Med 2012;18:1052–9.
49. Balko JM, Giltnane JM, Wang K, Schwarz LJ, Young CD, Cook RS, et al. Molecular profiling of the residual disease of triple-negative breast cancers after neoadjuvant chemotherapy identifies actionable therapeutic targets. Cancer Discov 2014;4:232–45.
50. Craig DW, O'Shaughnessy JA, Kiefer JA, Aldrich J, Sinari S, Moses TM, et al. Genome and transcriptome sequencing in prospective metastatic triple-negative breast cancer uncovers therapeutic vulnerabilities. Mol Cancer Ther 2013;12:104–16.
51. Maciejowski J, de Lange T. Telomeres in cancer: tumour suppression and genome instability. Nat Rev Mol Cell Biol 2017;18:175–86.
52. Xue Y, Marvin ME, Ivanova IG, Lydall D, Louis EJ, Maringele L. Rif1 and Exo1 regulate the genomic instability following telomere losses. Aging Cell 2016;15:553–62.
53. Alexandrov LB, Nik-Zainal S, Wedge DC, Aparicio SA, Behjati S, Biankin AV, et al. Signatures of mutational processes in human cancer. Nature 2013;500:415–21.
54. Nik-Zainal S, Davies H, Staaf J, Ramakrishna M, Glodzik D, Zou X, et al. Landscape of somatic mutations in 560 breast cancer whole-genome sequences. Nature 2016;534:47–54.

Published OnlineFirst October 10, 2018; DOI: 10.1158/1535-7163.MCT-18-0243

Molecular Cancer Therapeutics

A Four-gene Decision Tree Signature Classification of Triple-negative Breast Cancer: Implications for Targeted Therapeutics

Jelmar Quist, Hasan Mirza, Maggie C.U. Cheang, et al.

Mol Cancer Ther 2019;18:204-212. Published OnlineFirst October 10, 2018.